Protocols for the Miller indexing of Sb₂Se₃ and a non-x-ray method of orienting its single crystals.

T D C Hobson and K Durose
Stephenson Institute for Renewable Energy / Department of Physics, University of Liverpool, Chadwick Building, Peach St, Liverpool, L69 7ZF, United Kingdom.

Abstract

Sb_2Se_3 is a highly anisotropic semiconductor and unambiguous Miller indexing of its planes and diffraction patterns is therefore important – as is the preparation of oriented and indexed surfaces of single crystals for fundamental studies. The purpose of this letter is twofold: a) to bring attention to the two different Miller indexing conventions in popular use for Sb_2Se_3, (Space group Number 62, settings *Pnma* and *Pbnm*) explaining how they are related to its crystal structure and making recommendations for reporting protocols, and b) to draw attention to a non- x-ray method of preparing the three {100} type faces of single crystals of Sb_2Se_3 for use in physical investigations.

Introduction

Sb_2Se_3 is a mid-range bandgap semiconductor that is of current interest as an energy conversion material in solar photovoltaic cells [1, 2] and in photocatalysis [3] and water splitting [4].

Its structure has been reported in a number of original studies [5-9]: It adopts the orthorhombic crystal system, i.e. $a \neq b \neq c$ and $\alpha = \beta = \gamma = 90°$ and its most noticeable feature is that it comprises covalently bonded $(Sb_4Se_6)_n$ ribbons that are aligned parallel to the short axis of the unit cell, the ribbons being held in place by van der Waals interactions. This imparts significant anisotropy to its optical, [10] electrical and magnetic [11] properties. Moreover it has been postulated that enhanced photovoltaic response should be achievable using textured polycrystalline thin films for which the covalent ribbons are all aligned perpendicular to the plane of the film [2]. Hence the unambiguous labelling of the planes and directions is important in both basic science and applied reports on this material.

Nevertheless, two indexing conventions are in common use for Sb_2Se_3, these being *Pnma* and *Pbnm*, and a survey of twenty of the most recent papers on Sb_2Se_3 revealed a variety of reporting practice: Of these twenty, three [12-14] explicitly use the *Pnma* convention and three [15-17] the *Pbnm.* For a further nine [18-26] it is possible to infer that *Pnma* was used, and similarly for a further five [3, 27-30] for *Pbnm*. There is hence a rough 60/40 split between the two conventions, but for 70% overall additional knowledge is required to determine which convention was used. While there are occasional examples of good practice [16] there are rather more papers where it is not possible to determine the convention used, and occasionally both are used in the same paper. Below we explain the differences between the two conventions and make recommendations for those publishing in the field. In the second part of the letter we also draw attention to a lesser known method for preparing oriented {100} surfaces of Sb_2Se_3 crystals. Overall, the purpose of this letter is to provide a handy reference for researchers in order to avoid confusion about indexing, rather than to present original results.

Pnma and Pbnm indexing conventions and recommendations for reporting

Sb_2Se_3 adopts space group Number 62 (orthorhombic), for which there are six possible ways of presenting the crystal lattice on the **a, b** and **c** axes. These are: Settings 1 (*Pnma* using **a, b, c**, the standard setting), 2 (*Pmnb*, using **b, a, c̄**), 3 (*Pbnm*, using **c, a, b**), 4, (*Pcmn*, using **c, b, a**), 5 (*Pmcn*, using **b, c, a**) and 6 (*Pnam*, using **a, c̄, b**) [31].

Figure 1 shows the Sb_2Se_3 structure with the conventional axes for the two commonly used settings, *Pnma* and *Pbnm*, being shown alongside it, while Table 1 presents a summary of these two protocols. *Pnma* is widely used since it is 'setting 1' in the International Tables for Crystallography [31] - it allocates the covalent ribbon axis to the **b** vector i.e. [010]. The alternative, *Pbnm* is popular since it has the conceptual advantage of allocating the (unique) covalent ribbon axis to the **c** vector i.e. [001]. Both conventions are in regular use and rather than to recommend one over the other we instead present this letter to clarify the two conventions and to suggest the inclusion of a clear statement in published works.

Authors are recommended to include a statement similar to one of the following when publishing on Sb_2Se_3:

> "In this work we have used the space group #62 *Pnma* setting for the Miller indexing of planes in Sb_2Se_3 for which, a = 11.794, b = 3.986 and c = 11.648 Å and the covalently bonded ribbons lie parallel to the **b**-vector, [010]."

> or

> "In this work we have used the space group #62 *Pbnm* setting for the Miller indexing of planes in Sb_2Se_3 for which a = 11.648, b = 11.794 and c = 3.986 Å and the covalently bonded ribbons lie parallel to the **c**-vector, [001]."
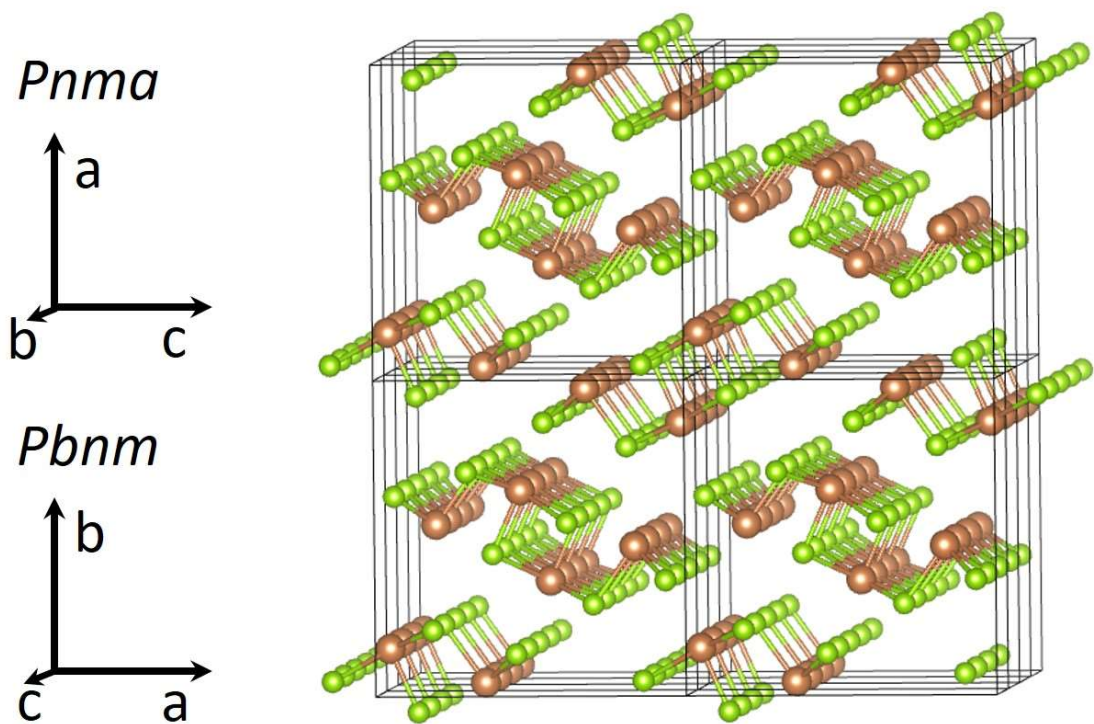
Figure 1. Diagram showing the two indexing conventions for space group number 62 alongside a 2 x 2 x 4 block of orthorhombic unit cells of Sb_2Se_3. Its structure comprises covalently bonded ribbons of $(Sb_4Se_6)_n$ coming out of the plane of the diagram. In 'setting 1', *Pnma*, a = 11.794, b = 3.986 and c = 11.648 Å and the ribbons lie parallel to the **b**-vector, [010]. In 'setting 3', *Pbnm*, a = 11.648, b = 11.794 and c = 3.986 Å and the ribbons lie parallel to the **c**-vector, [001]. Sb atoms are shown in brown; Se in green. The diagram was prepared using VESTA3 [32] using data from Tideswell [7] (Crystallographic Information File from [33]).

Lattice parameters (Å) $d_{Pnma, Pbnm}$	Lattice vectors, Miller indices of directions			
	Pnma		*Pbnm*	
$d_{100, 010}$ = 11.794	**a**	[100]	**b**	[010]
$d_{010, 001}$ = 3.986	**b**	[010]	**c**	[001]
$d_{001, 100}$ = 11.648	**c**	[001]	**a**	[100]

Table 1. Comparison of the two orthorhombic space group #62 setting conventions (*Pnma* and *Pbnm*) used most frequently in the literature for Sb_2Se_3.

Method for orienting single crystals of Sb₂Se₃ on its three {100} planes

In the second part of this communication we draw attention to a little-known method to orient single crystals of Sb_2Se_3 for use in research work. The usual method to prepare oriented and cut surfaces of single cystals is to first orient them on a goniometer using the Laue x-ray back reflection method, [34] and then to transfer the goniometer to a wafering saw. An alternative method devised by us [10] for Sb_2Se_3 allows preparation of the three {100} surfaces by making use of a property of its cleavage planes: Sb_2Se_3 cleaves easily and uniquely on a plane parallel to the ribbon axis, the plane being (100) (*Pnma*) or equivalently (010) (*Pbnm*). Furthermore, the cleavage planes always display linear and parallel cleavage steps that are visible by eye, these lying parallel to the ribbon axis, i.e. [010] (*Pnma*) or [001] (*Pbnm*), as shown in Figure 2. Hence the simple act of cleaving single crystals of Sb_2Se_3 is sufficient to define a known <100> direction on a known {100} plane, and this allows the other two {100} planes to be exposed by cutting either perpendicular or parallel to the cleavage steps. Figure 3 shows an example of the cleavage steps.
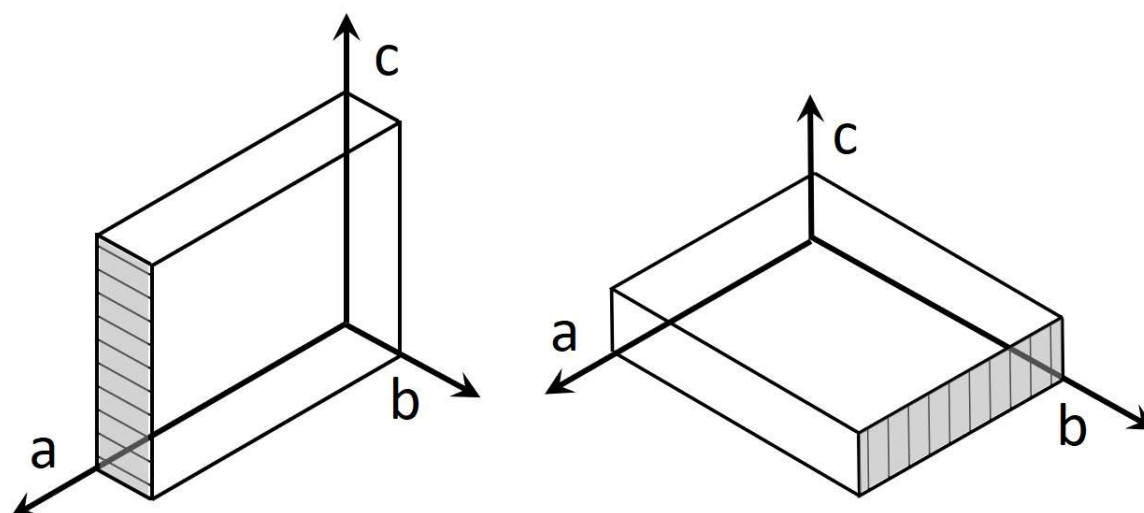
No 62, setting 1, *Pnma*
a = 11.794, b = 3.986, c = 11.648 Å
Ribbon axis is **b** = [010]
Cleavage plane is (100)
Cleavage steps lie on [010]

No 62, setting 3, *Pbnm*
a = 11.648, b = 11.794, c = 3.986 Å
Ribbon axis is **c** = [001]
Cleavage plane is (010)
Cleavage steps lie on [001]

Figure 2. Diagrams showing the indexing conventions for the orthorhombic unit cell having space group #62 using the *Pnma* and *Pbnm* settings. The shading indicates the cleavage plane for Sb_2Se_3, with the cleavage steps on it being indicated by parallel lines. These cleavage steps are oriented parallel to the covalent ribbons shown in Figure 1.
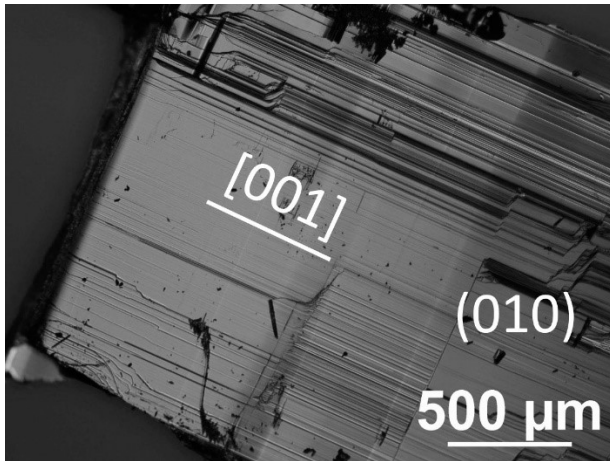
Figure 3. Optical micrograph of the cleavage plane of Sb_2Se_3 showing the cleavage steps. In the *Pbnm* setting shown on the diagram the cleavage plane is (010) and the cleavage steps lie along [001]. For *Pnma* (not shown), the cleavage plane is (100) and the steps lie on [010] directions.

The procedure for preparing (100), (010) and (001) surfaces of single crystals is therefore as follows:

For the *Pnma* convention.
    a) to prepare (100) cleave the crystal with a blade to reveal bright shiny (100) facets having visible cleavage steps aligned on [010].
    b) to prepare (010), first prepare a cleaved (100) surface and saw perpendicular to this surface and *perpendicular* to the cleavage steps.
    c) to prepare (001), first prepare a cleaved (100) surface and saw perpendicular to this surface and *parallel* to the cleavage steps.

For the *Pbnm* convention.
    i) the cleavage facets, (a) above, will be (010) with the cleavage steps lying on [001].
    ii) cutting perpendicular to the cleavage steps, (b) above, will give the (001) plane.
    iii) cutting parallel to the cleavage steps, (c) above, will give the (100) plane.

We prepared examples of all three {100} surfaces in this way from our own Bridgman-grown Sb_2Se_3 crystals [35] and examined them with θ - 2θ x-ray diffractometry, as shown in Figure 4. The broad diffuse background intensity arising from the glass sample holder was removed by manual selection in FULLPROF software [36].

In each case the diffraction patterns showed only peaks from a single plane and its higher order reflections i.e. a) (0*k*0), b) (00*l*) and c) (*h*00), with the positions of the reflections expected being shown by dotted lines calculated using the data from Tideswell [7] using VESTA software [32]. These results confirm the assertion made earlier that the cleavage steps lie parallel to the covalent ribbons, and also verify the methodology for preparing the three {100} surfaces. (We note incidentally that in Figure 4a, the 020 and 040 reflections are absent even though they are structure factor allowed and they have nevertheless been observed in ref. 10 for example. We attribute their absence to the stringency of alignment required for the excitation of Bragg reflections from single crystals, with alignment issues being exacerbated by the distortion (bending) of the crystal planes that is observed experimentally in Sb_2Se_3 and which will be the subject of a future report).
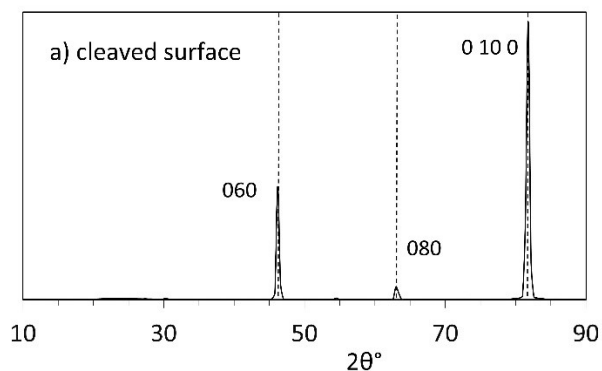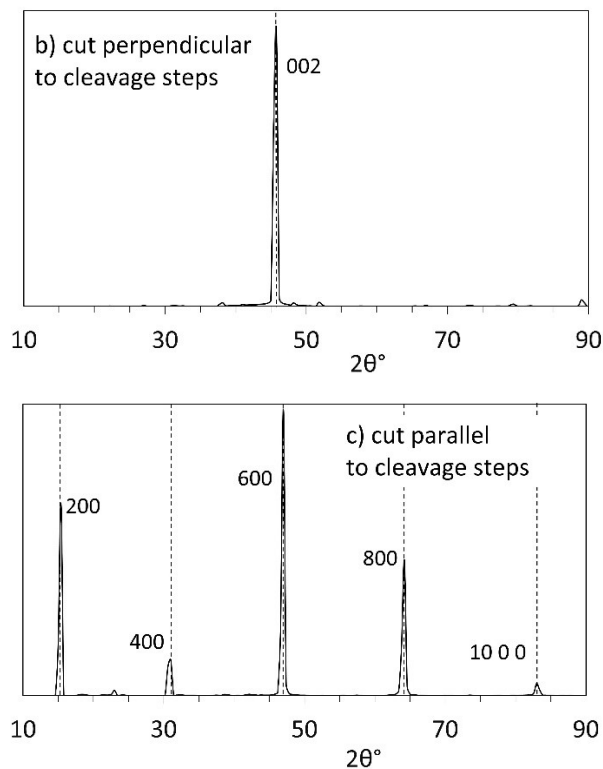
Figure 4. θ - 2θ XRD patterns of dice of Sb_2Se_3 single crystals oriented using the cleavage method described in the text. Reflections are indexed according to the *Pbnm* setting. a) the cleaved surface, (010), b) the surface cut perpendicular to the cleavage steps on the cleaved surface, (001) and c) cut parallel to the cleavage steps, (100). In each case only reflections for the selected planes and their higher order reflections are present. The patterns were recorded using a low-resolution mode of the diffractometer (Rigaku Smart Lab, CuKα$_{1,2}$) with a step interval of 0.4°, and hence the peak widths are not representative of the crystal perfection.

Summary

This letter has summarised and clarified the two Miller indexing conventions in common use for Sb_2Se_3, namely space group Number 62 setting 1 *Pnma* and setting 3 *Pbnm* as shown in Figures 1 and 2. For *Pnma* the covalent ribbon axis is [010] whereas for *Pbnm* it is [001]. Authors are encouraged to declare explicitly which convention they have used in their publications and recommended phrases are suggested above. Also, we have reported a non- x-ray method of orienting single crystals of Sb_2Se_3 based on the unique orientation of the cleavage plane and the cleavage steps on it, these being (100) [010] for *Pnma* and (010) [001] for *Pbnm*.

Acknowledgements

References

1. Nair, M.T.S., et al., *Chemically deposited thin films of sulfides and selenides of antimony and bismuth as solar energy materials*. Optical Materials Technology for Energy Efficiency and Solar Energy Conversion XV, ed. C.M. Lampert, et al. Vol. 3138. 1997, Bellingham: SPIE - Int Soc Optical Engineering. 186-196.
2. Zhou, Y., et al., *Thin-film Sb_2Se_3 photovoltaics with oriented one-dimensional ribbons and benign grain boundaries.* Nature Photonics, 2015. **9**(6).
3. Ren, D.L., et al., *In situ synthesis and improved photoelectric performances of a Sb_2Se_3/beta-In_2Se_3 heterojunction composite with potential photocatalytic activity for methyl orange degradation.* Ceramics International, 2020. **46**(16): p. 25503-25511.
4. Yang, W., et al., *Benchmark performance of low-cost Sb_2Se_3 photocathodes for unassisted solar overall water splitting.* Nature Communications, 2020. **11**(1): p. 10.
5. Donges, E., *Uber-chalkogenohalogenide des dreiwertigen antimons und wismuts 2. Uber selenohalogenide des driwertigen antimons und wismuts und uber antimon(III)-selenid.* Zeitschrift fur Anorganische Chemie, 1950. **263**(5-6): p. 280-291.
6. Donges, E., *Uber chalkogenohaogenide des dreiwertigen antimons und wismuts 3. Uber tellurohalogenide des dreiwertigen antimons und wismuts uber antimon-tellurid und wismut(III)-tellurid und wismut(III)-selenid.* Zeitschrift fur Anorganische und Allgemeine Chemie, 1951. **265**(1-3): p. 56-61.
7. Tideswell, N.W., F.H. Kruse, and J.D. McCullough, *The crystal structure of antimony selenide, Sb_2Se_3.* Acta Crystallographica, 1957. **10**(2): p. 99-102.
8. Voutsas, G.P., et al., *The crystal-structure of antimony selenide, Sb_2Se_3.* Zeitschrift fur Kristallographie, 1985. **171**(3-4): p. 261-268.
9. Caracas, R. and X. Gonze, *First-principles study of the electronic properties of A(2)B(3) minerals, with A=Bi,Sb and B=S,Se.* Physics and Chemistry of Minerals, 2005. **32**(4): p. 295-300.
10. Fleck, N., et al., *Identifying Raman modes of Sb_2Se_3 and their symmetries using angle-resolved polarised Raman spectra.* Journal of Materials Chemistry A, 2020. **8**(17): p. 8337-8344.
11. Chakraborty, B.R., et al., *Magnetic and electric properties of antimony selenide (Sb_2Se_3) crystals.* Journal of Physics and Chemistry of Solids, 1980. **41**(8): p. 913-917.
12. Wang, J.L., et al., *Solution-processed Sb_2Se_3 on TiO_2 thin films toward oxidation-and moisture-resistant, self-powered photodetectors.* ACS Applied Materials & Interfaces, 2020. **12**(34): p. 38341-38349.
13. Syrbu, N.N., et al., *Excitonic and electronic transitions in Me-Sb_2Se_3 structures.* Beilstein Journal of Nanotechnology, 2020. **11**: p. 1045-1053.
14. Peng, X.B., et al., *Theoretical investigation of the electronic structure and anisotropic optical properties of quasi-1D Sb_2Se_3 photovoltaic absorber materials.* in press in Journal of Computational Electronics. Published online 20 October 2020 doi: 10.1007/s10825-020-01595-2
.
15. Tiwari, K.J., et al., *Efficient Sb_2Se_3/CdS planar heterojunction solar cells in substrate configuration with (hk0) oriented Sb_2Se_3 thin films.* Solar Energy Materials and Solar Cells, 2020. **215**: p. 8.
16. Pattini, F., et al., *Role of the substrates in the ribbon orientation of Sb_2Se_3 films grown by low-temperature pulsed electron deposition.* Solar Energy Materials and Solar Cells, 2020. **218**: p. 10.
17. Guan, F., et al., *Oleic acid-induced, controllable surface oxidation to enhance the photoresponse performance of Sb_2Se_3 nanorods.* CrystEngComm, 2020. **22**(37): p. 6189-6194.

18.   Zhou, H.P., et al., *Fabrication of a preferentially 001-oriented Sb₂Se₃ thin film on diverse substrates and its application in photoelectrochemical water reduction.* Sustainable Energy & Fuels, 2020. **4**(8): p. 3943-3950.

19.   Yang, K., B. Li, and G.G. Zeng, *Structural, morphological, compositional, optical and electrical properties of Sb₂Se₃ thin films deposited by pulsed laser deposition.* Superlattices and Microstructures, 2020. **145**: p. 7.

20.   Wen, X.X., et al., *High-crystallinity epitaxial Sb₂Se₃ thin films on mica for flexible near-infrared photodetectors.* ACS Applied Materials & Interfaces, 2020. **12**(31): p. 35222-35231.

21.   Wen, S., et al., *Vapor transport deposition of Sb₂Se₃ thin films for photodetector application.* Journal of Advanced Dielectrics, 2020. **10**(4): p. 6.

22.   Ren, D.L., et al., *Fundamental physical characterization of Sb₂Se₃ -based quasi-homojunction thin film solar cells.* ACS Applied Materials & Interfaces, 2020. **12**(27): p. 30572-30583.

23.   Mavlonov, A., et al., *Structural and morphological properties of PLD Sb₂Se₃ thin films for use in solar cells.* Solar Energy, 2020. **208**: p. 451-456.

24.   Liang, X.Y., et al., *Crystallographic orientation control of 1D Sb₂Se₃ nanorod arrays for photovoltaic application by in situ back-contact engineering.* Solar RRL, 2020. **4**(10): p. 8.

25.   Huang, M.L., Z.H. Cai, and S.Y. Chen, *Quasi-one-dimensional Sb₂(S,Se)₃ alloys as bandgap-tunable and defect-tolerant photocatalytic semiconductors.* Journal of Chemical Physics, 2020. **153**(1): p. 7.

26.   Grad, L., et al., *Photoexcited charge carrier dynamics in Sb₂Se₃ (100).* Physical Review Materials, 2020. **4**(10): p. 9.

27.   Wang, S.J., et al., *A stable conversion and alloying anode for potassium-ion batteries: a combined strategy of encapsulation and confinement.* Advanced Functional Materials, 2020. **30**(27): p. 10.

28.   Shi, W.J., et al., *Antimony selenide thin film solar cells with an electron transport layer of Alq(3).* Chinese Physics Letters, 2020. **37**(10): p. 6.

29.   Ren, D.L., et al., *Structure, morphology, and photoelectric performances of Te-Sb₂Se₃ thin film prepared via magnetron sputtering.* Nanomaterials, 2020. **10**(7): p. 13.

30.   Luo, Y.D., et al., *An effective combination reaction involved with sputtered and selenized Sb precursors for efficient Sb₂Se₃ thin film solar cells.* Chemical Engineering Journal, 2020. **393**: p. 12.

31.   Bertaut, E.F., *Synoptic tables for space-group symbols, Table 4.3.2.1.*, in *International Tables for Crystallography*. 2002, Springer.

32.   Momma, K. and F. Izumi, *VESTA 3 for three-dimensional visualization of crystal, volumetric and morphology data.* Journal of Applied Crystallography, 2011. **44**: p. 1272-1276.

33.   *Crystallography Open Database.* [CIF file 9007437.cif] [accessed 24 November 2020].

34.   Barrett, C. and T.B. Massalski, *The Structure of Metals: Crystallographic Methods, Principles, and Data*. 3rd ed. 1980: Pergamon.

35.   Hobson, T.D.C., et al., *Growth and characterization of Sb₂Se₃ single crystals for fundamental studies*, in *2018 IEEE 7th World Conference on Photovoltaic Energy Conversion*. 2018, IEEE: New York. p. 0818-0822.

36.   Rodríguez-Carvajal, J., *Recent Developments of the Program FULLPROF* Commission on Powder Diffraction (IUCr) Newsletter, 2001. **26**: p. 12 - 19 (The complete program and documentation can be obtained in http://www.ill.eu/sites/fullprof/)